

RESEARCH PAPER

Palm tree structured wide band monopole antenna

SANDEEP K. PALANISWAMY¹, KANAGASABAI MALATHI¹ AND ARUN K. SHRIVASTAV²

This paper presents design, fabrication, and testing of a palm tree structured monopole antenna for wideband applications. The proposed antenna has a wide impedance bandwidth (−10 dB bandwidth) from 4 to 10.4 GHz. Palm tree antenna of compact size 23 mm × 20 mm is designed and fabricated on an FR4 substrate of thickness 1.6 mm. To validate the design, a mathematical relationship between the parameters of the palm tree geometry and the lower cut-off frequency has been established. Parametric study has been carried out to obtain optimum wideband characteristics. The prototype is experimentally validated for the band 4–10.4 GHz within ultra-wideband operations. Transfer function, impulse response and Group delay has been plotted in order to address the time domain characteristics of the palm tree antenna with fidelity factor values. The possible applications cover 5.2–5.8 GHz WLAN, C-band operations, 5.5 GHz WiMAX, and Wireless USB.

Keywords: Antenna design, Modeling and measurements, Antennas and propagation for wireless systems

Received 20 January 2015; Revised 13 February 2015; Accepted 15 February 2015; first published online 30 March 2015

I. INTRODUCTION

Ultra-wideband (UWB) was approved by the Federal Communications Commission (FCC) for unlicensed operation in the 3.1–10.6 GHz band [1]. The transmitted signal must instantaneously occupy either a fractional bandwidth in excess of 20% of the center frequency or in excess of 500 MHz of absolute bandwidth to be classified as a UWB signal.

The prime issue in UWB communication systems is the design of a compact antenna providing wideband characteristics. In this regard, a number of planar monopoles with different structures like U-shaped, circular, elliptical, and triangular patches have been reported. The reported several shaped radiators have extended their study to enhance characteristics of compactness, omni-directional radiation pattern and wideband characteristics [2–12]. Other strategies to improve the impedance bandwidth have also been investigated [13, 14]. On the other hand, in [15–17], the designs have complicated structures that lead to an increase in fabrication costs, antenna size, and difficulty in integration with microwave-integrated circuits. A mathematical relationship has been established and presented for lower band-edge frequency for all the regular shapes of printed monopole antennas with various feed positions [18, 19].

In this paper, a new palm tree structured printed monopole antenna is presented. First an ellipse was created and then it was made to rotate about the origin with an angle of 15° to obtain 19 elliptical structures over a widespread of 270° in

the radiating plane and finally fused to form the palm tree geometry which achieves a wideband performance, providing a bandwidth from 4 to 10.4 GHz. The proposed antenna has a low profile of 23 mm × 20 mm, and is one of the compact antennas reported [2, 3, 6–9, 11–13, 20–26]. The antenna can be used for Wireless Local Area Network (WLAN), Worldwide interoperability for Microwave Access (WiMAX), wireless USB, and C-band operations. In this work, complete frequency-domain and time-domain analysis have been performed for the proposed palm tree structured monopole antenna. The proposed palm tree structured antenna is of small and compact size with wideband from 4 to 10.4 GHz, gain ranging from 2 to 5.9 dBi, group delay variation less than 0.25 ns and average fidelity factor of 0.77.

This paper consists of five sections. Section I briefs the introduction, Section II deals with antenna design and configuration. Section III contains results and discussions, which involves parametric study; Section IV is comparison of simulated results and measured results and the time-domain analysis of the antenna. Section V concludes the work.

II. ANTENNA DESIGN AND CONFIGURATION

The proposed planar monopole antenna fed by a microstrip line is shown in Fig. 1, which is printed on an FR4 substrate of thickness 1.6 mm, permittivity of 4.3, and loss tangent 0.025. The basic palm tree monopole antenna structure consists of a palm tree geometry (fusion of various rotated ellipses), a microstrip feed line, and a ground plane. The prototype is connected to a 50-Ω SubMiniature version A (SMA) connector.

Figure 1 shows the antenna schematic and is based on a monopole design. The width of the microstrip feed W_1 is

¹Department of Electronics and Communication Engineering, College of Engineering, Guindy Campus, Anna University, Chennai 600 025, India

²Center for Electromagnetics, SAMEER, Taramani, Chennai, India

Corresponding author:

P. S. Kumar

Email: vrpchs@gmail.com

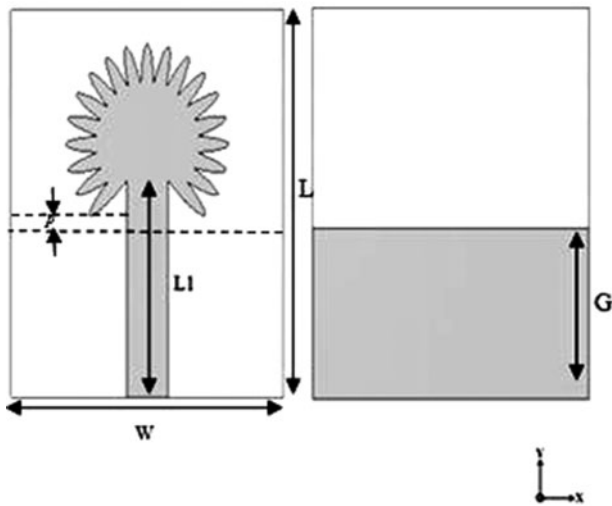


Fig. 1. The palm tree antenna front and rear view.

fixed at 3 mm and the length of the microstrip feed L_1 is fixed at 15 mm, to match 50Ω impedance and to achieve an optimum bandwidth, respectively. The semi-major axis length X and semi-minor axis length Y of the ellipse are 3 and 0.5 mm, respectively. The ground plane is provided below the feed in the rear plane and the optimum length G is 10 mm. The overall dimension $L \times W$ of the antenna is 23 mm \times 20 mm.

$$f_1 = \frac{7.2}{(l + r + p) \times k} \tag{1}$$

Equation (1) is worked out for the planar monopole antennas as referred in [15, 16]. In (1), f_1 is the lower band-edge frequency in GHz, l is the height of the planar monopole antenna in cm, which is taken same as that of an equivalent cylindrical monopole and r in cm, the effective radius of the equivalent cylindrical monopole antenna, which is determined by equating area of the planar and cylindrical monopole antennas, p in cm is the distance between the ground plane and the radiator and k is the factor which is having similar significance as $\sqrt{(\epsilon_{eff})}$. The empirical value of k is 1.2758. The lower band-edge frequency for the palm tree structured prototype in GHz is given as

$$f_1 = \frac{7.2}{(1.194\pi(X + Y) + p) \times k} \tag{2}$$

In Equation (2), X and Y are the length of semi-major and semi-minor axis of the ellipses in the palm tree structure in cm, respectively. For the proposed palm tree antenna ($l + r$) term is related to $(1.194\pi(X + Y))$.

III. PARAMETRIC STUDY

In this section, the parameters of this proposed antenna are studied by changing one parameter at a time and keeping the other parameters unchanged. As the length L_1 and width W_1 of the microstrip feed has been fixed for impedance matching, the optimal parameters taken for the study are the ground plane length G (in mm fixing $X = 3$ mm, $Y = 0.5$ mm, and $p = 0.8$ mm), the length of semi major axis X of the ellipse

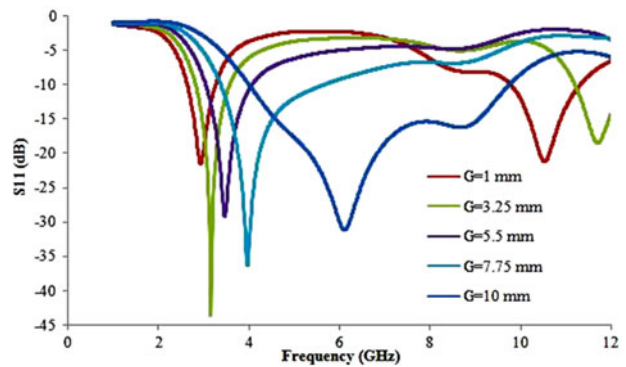


Fig. 2. The reflection coefficient characteristics of various ground plane distances G of the palm tree geometry (in mm).

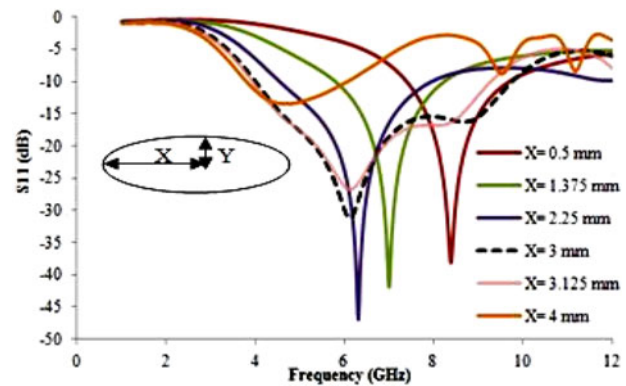


Fig. 3. The reflection coefficient characteristics of various semi major axis length X of the ellipse in the palm tree geometry (in mm).

(in mm keeping semi minor axis $Y = 0.5$ mm), the number of ellipses n and the variation of the angle theta of the ellipses created over the 270° in the radiating plane (fixing $X = 3$ mm, $Y = 0.5$ mm, $p = 0.8$ mm, and $G = 10$ mm) in the antenna structure. Figures 2 and 3 show the variations of reflection coefficient for different values of G and the length of semi-major axis X of the ellipse, respectively. In Fig. 2, it is observed that when G is increased from 1 to 10 mm, the bandwidth increases and the frequency shift occurs. Therefore at $G = 10$ mm an optimum bandwidth from 4 to 10.2 GHz has been obtained.

Table 1 lists various G and X values (in mm) swept to view their effect on the f_1 lower band-edge frequency in GHz. In Fig. 3, the length of semi-major axis X of the ellipse in the palm tree structure is varied and is increased from 0.5 to 4 mm (keeping G as a constant 10 mm), the bandwidth increases and the frequency shift occurs. Therefore at a semi-major axis length X of 3 mm, a wide bandwidth from 4 to 10.2 GHz was obtained and semi-major axis length X of 3 mm was inferred as the optimum semi-major axis length. As shown in Table 1 the parametric study for X is done, to ensure that at $X = 3$ mm, $Y = 0.5$ mm, and $p = 0.8$ mm, the f_1 is equal to 4.05 GHz as per (2). It is also noted that for all the other values of X , p varies as X increases, so as to satisfy (2). In order to avoid the overlap of the ground and radiator, the p value must be positive and X can take a maximum value up to 3.343 mm for a fixed $Y = 0.5$ mm and $p = 0.01$ mm. If there is overlap between the radiator and the ground, the value of p becomes negative and a wideband cannot be achieved. For example, when $X = 4$ mm, the value of p is -1.98 mm as seen

Table 1. Parametric study

Parameter	Values (mm)	f_l (lower band-edge frequency in GHz)
G ($X = 3$ mm, $Y = 0.5$ mm, $p = 0.8$ mm)	1	2.64
	3.25	2.82
	5.5	3.05
	7.75	3.39
	10	4.05
X, p ($Y = 0.5$ mm, p varies with X as p is the distance between the radiator and the Ground plane)	0.500, 3.800	7.39
	1.375, 2.686	5.81
	2.250, 2.150	4.53
	3.000, 0.814	4.05
	3.125, 0.735	3.94
	4.000, -1.980	3.79

in Table 1 and it is verified that at $X = 4$ mm there exists ripples and a wideband is not achieved as shown in Fig. 3.

First an ellipse was created and then it was made to rotate about the origin with an angle θ of 45° , 22.5° , 15° , and 7.5° to obtain 7, 13, 19 and 37 elliptical structures, respectively, over a widespread of 270° in the radiating plane and finally fused to form various palm tree geometries fixing $X = 3$ mm, $Y = 0.5$ mm, $p = 0.8$ mm, and $G = 10$ mm. Figure 4 shows the reflection coefficient characteristics of various θ values (in degrees) and number of ellipses in the palm tree geometry. In Fig. 4, it is noted that for theta of 15° and for nineteen number of ellipses in the palm tree geometry, the bandwidth is achieved from 4 to 10.2 GHz. It is also observed that for various number of ellipses and the variation of θ in the palm tree geometry over a wide spread of 270 degrees in the radiating plane, the lower band-edge frequency f_l remains the same at

4 GHz. The parametric study shown in Figs 2 and 3 corresponds to $n = 19$ elliptical structures. Therefore an ellipse was created and then it was made to rotate about the origin with an angle of 15° to obtain $n = 19$ elliptical structures over a widespread of 270° in the radiating plane and finally fused to form the palm tree geometry which achieves an optimum wideband performance from 4 to 10.2 GHz.

IV. MEASURED RESULTS AND DISCUSSIONS

Figure 5 shows the simulated and measured reflection coefficient ($|S_{11}|$) characteristics. It is clearly seen that the palm tree antenna has a wide impedance bandwidth (at -10 dB of $|S_{11}|$) from 4 to 10.2 GHz in simulated and in measured the bandwidth (at -10 dB of $|S_{11}|$) from 4 to 10.4 GHz was obtained. From the simulated and measured reflection coefficient results shown in Fig. 4 and from Table 1, the lower band-edge frequency is $f_l = 4$ GHz, which agrees well with the calculated value with the help of (2). Measured reflection coefficient ($|S_{11}|$) of the designed antenna matches reasonably with the simulation results. In the measured results, there exists some undulations which may be due to the limitations of the SMA port used, fabrication tolerances and the small size of the backing ground plane compared with the connected cable which completely modifies the currents distribution [25]. The measured reflection coefficient of the antenna has been reduced, due to minute errors in the fabrication process (cutting off edges of the palm tree geometry).

Figure 6 depicts the simulated and measured radiation pattern of the aforementioned antenna in the xz -plane. Figure 7 illustrates the gain and radiation efficiency variations for various frequencies. It is noted that the gain ranges from 2 to 5.9 dBi and the radiation efficiency varies from -1 to -2 dB in the operating band from 4 to 10.4 GHz.

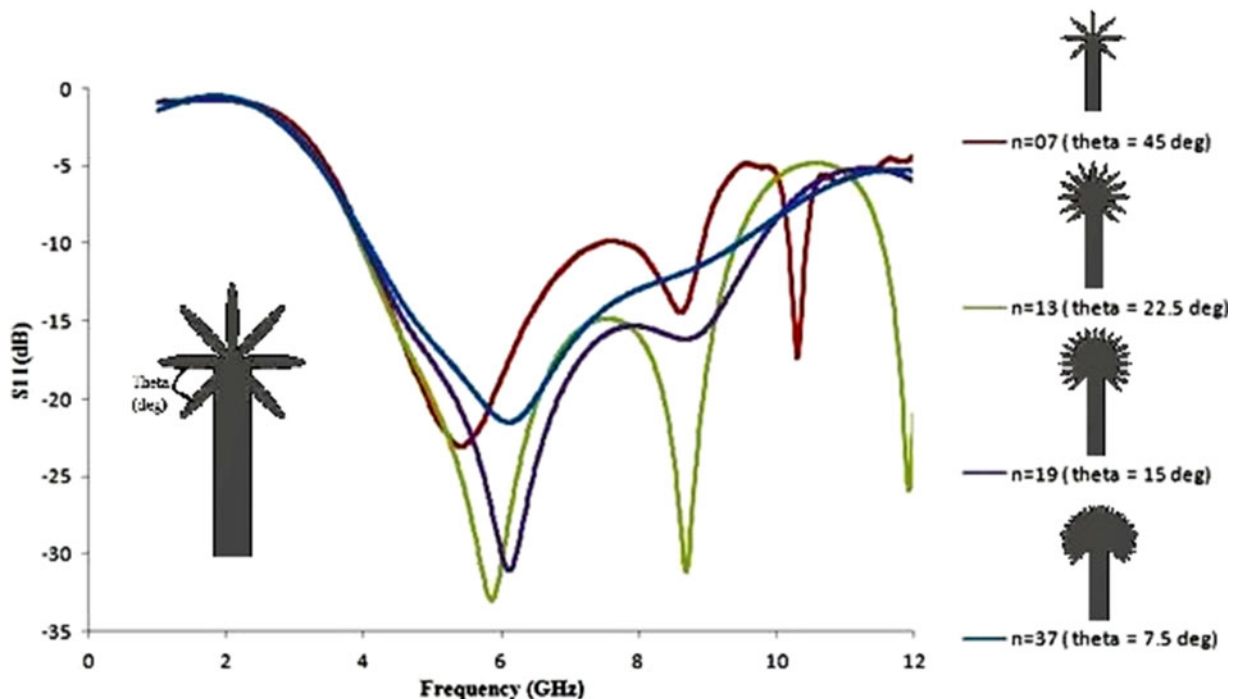


Fig. 4. The reflection coefficient characteristics of various theta values (in degrees) and number of ellipses in the palm tree geometry.

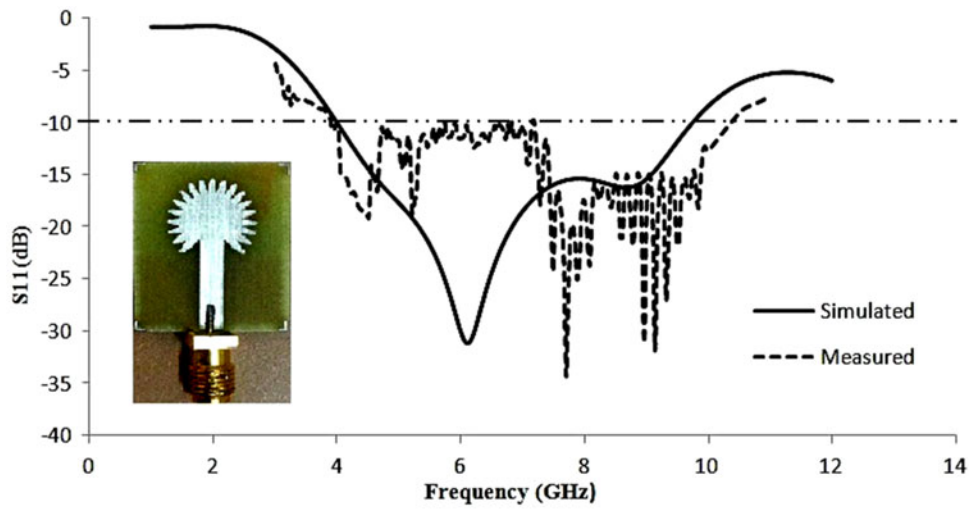


Fig. 5. Simulated and measured reflection coefficient characteristics of the palm tree antenna.

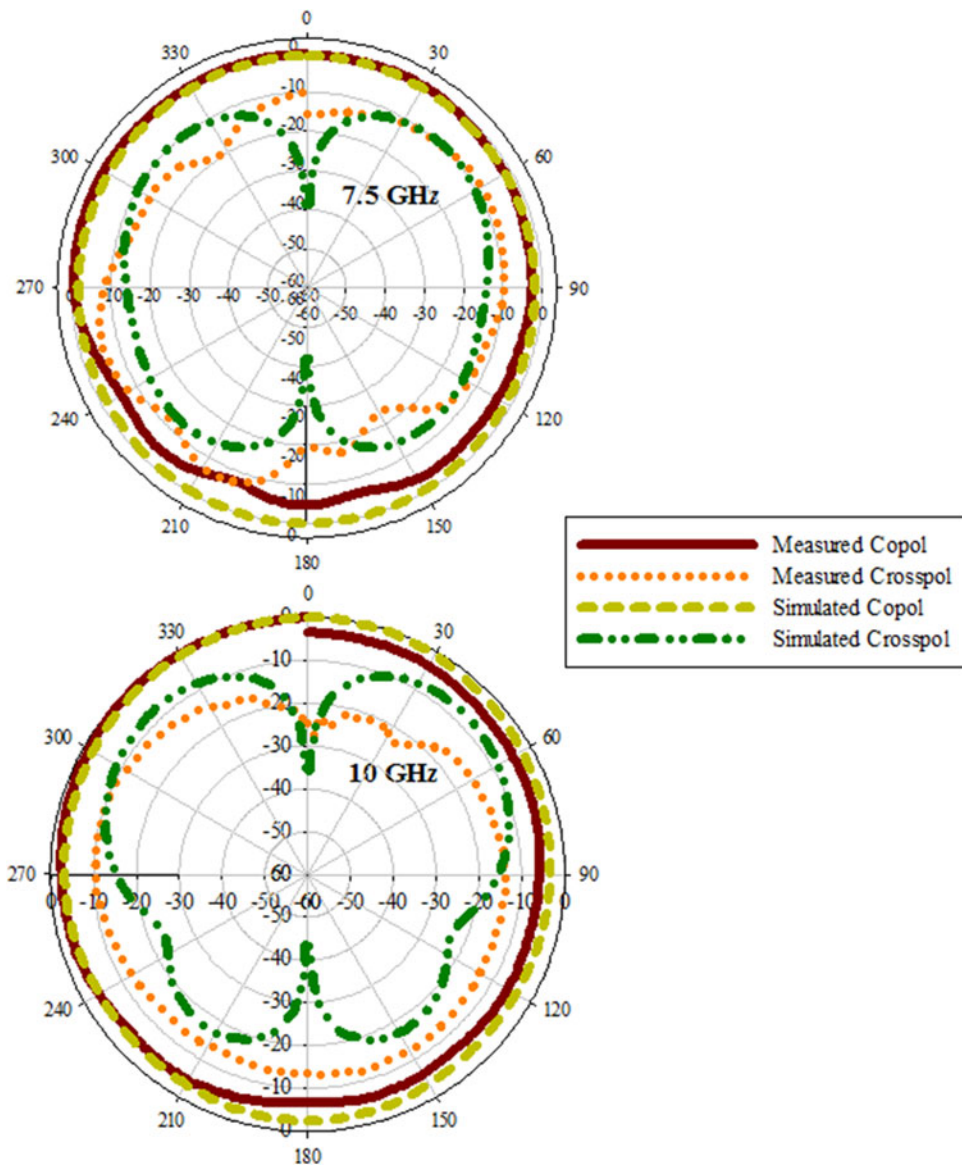


Fig. 6. Simulated and measured radiation patterns (xz -plane) for the frequencies 7.5 and 10 GHz, respectively.

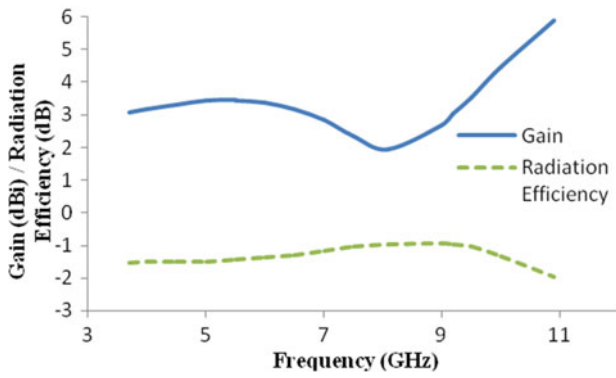


Fig. 7. Gain (in dBi) and radiation efficiency (in dB) versus frequency (GHz).

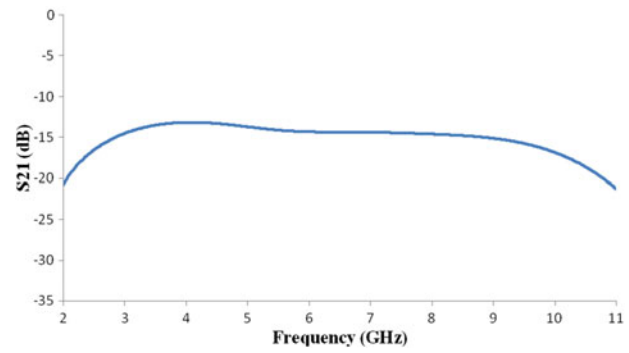


Fig. 8. Magnitude of transfer function ($|S_{21}|$) (Plotted when two identical palm tree-shaped antennas (transmitter and receiver) are placed with a separation distance of 100 mm.).

UWB systems use narrow pulses of very short duration for transmitting signals. Hence, the transfer function is crucial to evaluate the proposed antenna performance for efficient transmission of such pulses. By considering the antenna system as a two-port network, the transmission scattering parameter S_{21} of the antenna is plotted in simulation [27, 28]. Two antennas (transmitter and receiver) are placed with a separation distance of 100 mm in a face-to-face and side-to-side orientation for measuring the transmission characteristics and the pulse handling capability of the proposed antenna. Transmitter antenna functions as Port 1 and Receiver antenna functions as Port 2. The transmission characteristics between them is recorded and plotted. The simulated magnitude and phase of the transmission scattering parameter which indicates the antenna transfer function are shown in Figs 8 and 9. The magnitude of the transfer function should be frequency flat over the operation band. The magnitude plot of transfer function of the proposed antenna shows that it is nearly flat over the operating band from 4 to 10.4 GHz. Similarly, the phase of transfer function $\angle S_{21}$ should vary linearly over the operation band [27]. Transfer function phase $\angle S_{21}$ of the proposed antenna is perfectly linear over the entire band. From the magnitude and phase plots of the transfer function, the proposed antenna is suitable for wideband pulse communications.

Furthermore, to measure the pulse handling capability of the proposed palm tree structured antenna, time-domain

analysis was carried out with fidelity factor calculation using (3). The Transmitter is excited by a Gaussian signal (3.1–10.6 GHz) and the received signal is obtained. Transmitted and received signals are shown in Fig. 10. The fidelity factors in the case of face – face and side – side are obtained as 0.7932 and 0.7133, respectively. The input pulse and the received pulse of the antenna are shown in the same graph so as to compare the input and received pulse shapes. From Fig. 10, it can be seen that the received pulse almost preserves the pulse shape of the excited input pulse. The normalization is done in order to compare only the shape of the pulses, and not their magnitude, as the received signal R_s is expected to be much lower than the transmitted pulse T_s . The cross-correlation between both signals is done at every point in time and the maximum value is obtained as fidelity factor when both pulses overlap [29] and is given by

$$\text{Fidelity factor} = \max \int_{-\infty}^{+\infty} \widehat{T}_s(t) \widehat{R}_s(t + \tau) dt \quad (3)$$

Figure 11 illustrates the time-domain setup, where the transmitter and receiver antenna are placed with a separation of 100 mm and “ φ ” is the angle of rotation (in degrees) of the receiver antenna. For various angles of rotation, the fidelity factor was obtained and is tabulated in Table 2. From Table 2, the average fidelity of 0.7716 is obtained, which is higher than the commonly accepted minimum value of 0.5 [29].

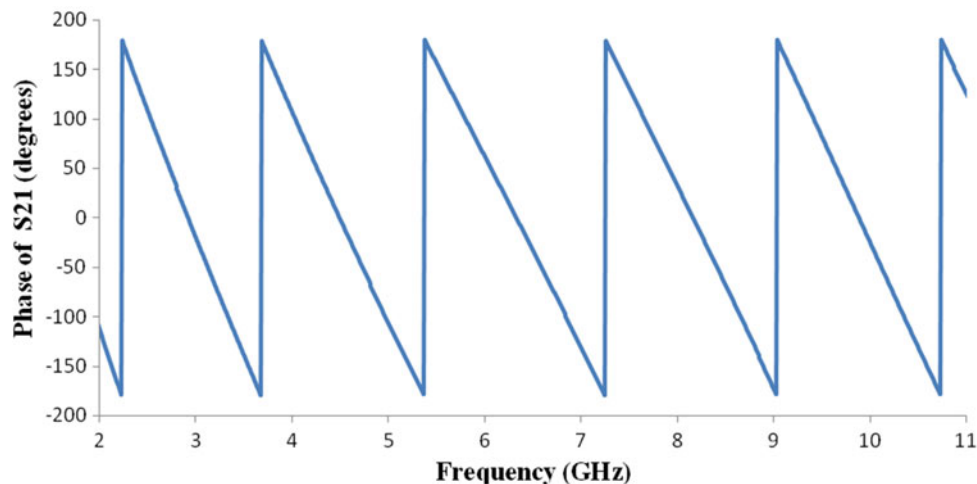


Fig. 9. Phase of transfer function ($\angle S_{21}$) (Plotted when two identical palm tree-shaped antennas (transmitter and receiver) are placed with a separation distance of 100 mm.).

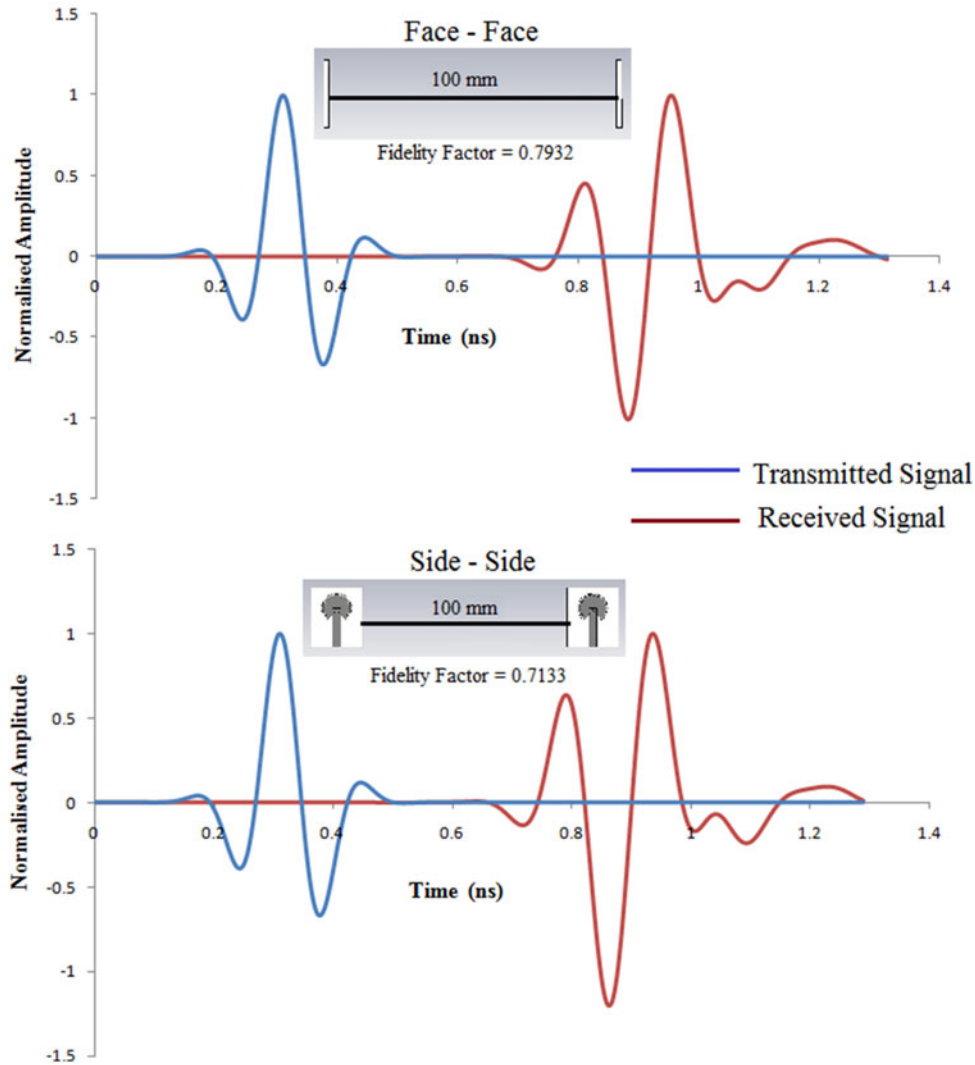


Fig. 10. Transmitted and received signals with face – face and side – side orientations with fidelity factor of the proposed antenna.

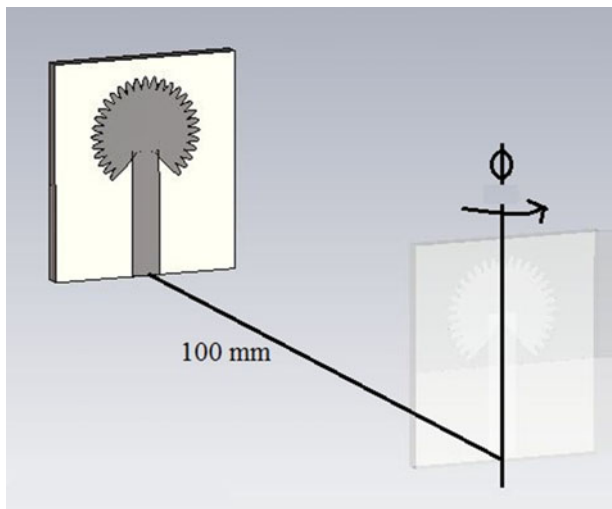


Fig. 11. Transmitter and receiver antenna arrangement. (“ ϕ ” is the angle of rotation of the receiver antenna).

Group delay is another important parameter to characterize the wideband antenna behavior, which measures the degree of distortion of signal waveforms. The Group delay

graph of the palm tree antenna is illustrated in Fig. 12. It is noted that the Group delay of the antenna is almost flat over the entire operating band in the UWB frequency range.

Table 2. Fidelity factor

Φ (degrees)	0°	90°	180°	270°
Fidelity factor	0.7932	0.7437	0.8160	0.7335

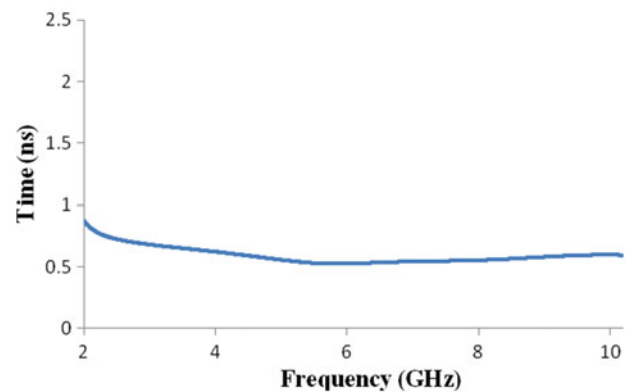


Fig. 12. Group delay of the palm tree antenna.

Table 3. Performance comparison

Ref. no.	Substrate used	Frequency band (GHz)	Antenna dimension (mm ³)	Gain (dBi)	Group delay variation	Fidelity factor (avg.)
[2]	RT/Duroid 5880	4.6–10.3	29 × 26 × 2.36	4.48 (avg.)	Not reported	Not reported
[3]	Ro4003	3–11	30 × 25 × 0.5	1.4–4.6	Not reported	Not reported
[6]	FR4	2.7–10.5	24 × 28 × 1.6	Not reported	Not reported	Not reported
[7]	RT/Duroid 5880	3–11.43	41 × 18 × 1.575	3.43–5.27	Not reported	Not reported
[8]	FR4	2.4–24.3	41 × 30 × 0.5	0.7–4.4	Not reported	Not reported
[9]	FR4	2.8–9.8	42 × 50 × 1.5	3.5–6.7	Not reported	Not reported
[11]	TLC-30	2.62–15.45	40 × 35 × 1.575	4.5 (max.)	Not reported	Not reported
[13]	FR4	3.4–11	16 × 18 × 1.6	5.26 (max.)	Not reported	Not reported
[20]	FR4	2.6–10.04	25 × 25 × 1.6	Not reported	~1 ns	Not reported
[21]	FR4	3.7–10.1	24 × 20 × 1	2–7.3	~0.5 ns	0.9
[22]	FR4	3.1–10.6	25 × 33 × 1.14	5 (max.)	Not reported	Not reported
[24]	FR4	3.1–10	30 × 40 × 1.59	Not reported	Not reported	Not reported
[26]	FR4	1.5–11	60 × 56 × 1.6	4–8.1	Not reported	Not reported
Proposed work	FR4	4–10.4	23 × 20 × 1.6	2–5.9	~0.25 ns	0.77

The variation in time or delay of the frequency components of the signal is <0.25 ns for the entire operating band. It is constant for all frequencies which shows that all frequency components of the transmitted pulse remain intact, shows the better performance of the proposed antenna in terms of wideband characteristics compared with many other antennas in the literature [20, 30]. Table 3 lists the performance comparison of various prototypes. As seen in Table 3, the proposed antenna is one of the compact antenna in comparison with other prototypes in the literature. The palm tree structured antenna is of small and compact size with bandwidth 6.4 GHz, gain ranging from 2 to 5.9 dBi, group delay variation <0.25 ns, and average fidelity factor of 0.77.

V. CONCLUSION

This paper has been presented with a palm tree structured monopole antenna for wideband applications. From the results it is evident that the palm tree antenna has a wide impedance bandwidth (at -10 dB of $|S_{11}|$) from 4 to 10.4 GHz within the UWB frequency range. The designed antenna has a low profile, simple configuration, and low cost. Measured reflection coefficient ($|S_{11}|$) and measured radiation pattern of the designed antenna agree reasonably well with the simulation results. The calculations by the mathematical expression established for the lower band-edge frequency holds good and match with the simulated and measured results. The design exhibits constant group delay, flat transfer functions, and phase linearity. The time-domain analysis shows that the proposed antenna can be a potential candidate for wideband pulse communications.

ACKNOWLEDGEMENT

This work was supported by the Anna Centenary Research Fellowship, College of Engineering Guindy, Anna university, Chennai 600025, India.

REFERENCES

- [1] Federal Communications Commission: "First report and order". Revision of part 15 of the commission's rules regarding ultrawideband transmission systems, 2002.
- [2] Ren, Y.J.; Chang, K.: Ultra-wideband planar elliptical ring antenna. *Electron. Lett.*, **42** (8) (2006), 447–449.
- [3] Joon, I.K.; Yong, J.: Design of ultra wideband coplanar waveguide-fed LI-shape planar monopole antennas. *IEEE Antennas Wireless Propag. Lett.*, **6** (2007), 383–387.
- [4] Abbosh, A.S.; Bialkowski, M.E.: Design of ultra wideband planar monopole antennas of circular and elliptical shape. *IEEE Trans. Antennas Propag.*, **56** (1) (2008), 17–23.
- [5] Gopikrishna, M.; Krishna, D.D.; Aanandan, C.K.; Mohanan, P.; Vasudevan, K.: Compact linear tapered slot antenna for UWB applications. *Electron. Lett.*, **44** (20) (2008), 1174–1175.
- [6] Moghadasi, M.N.; Roustaei, H.; Virdee, B.S.: Compact UWB planar monopole antenna. *IEEE Antennas Wireless Propag. Lett.*, **8** (22) (2009), 1382–1385.
- [7] Ahmed, O.; Sebak, A.R.: A printed monopole antenna with two steps and a circular slot for UWB applications. *IEEE Antennas Wireless Propag. Lett.*, **7** (2008), 411–413.
- [8] Deng, C.; Xie, Y.J.; Li, P.: CPW-fed planar printed monopole antenna with impedance bandwidth enhanced. *IEEE Antennas Wireless Propag. Lett.*, **8** (2009), 1394–1397.
- [9] Liang, J.; Chiau, C.C.; Chen, X.; Parini, C.G.: Study of a printed circular disc monopole antenna for UWB systems. *IEEE Trans. Antennas Propag.*, **53** (11) (2005), 3500–3504.
- [10] Nguyen, D.T.; Lee, D.H.; Park, H.C.: Very compact printed triple band-notched UWB antenna with quarter-wavelength slots. *IEEE Antennas Wireless Propag. Lett.*, **11** (2012), 411–414.
- [11] Angelopoulos, E.S.; Anastopoulos, A.Z.; Kaklamani, D.I.; Alexandridis, A.A.; Lazarakis, F.; Dangakis, K.: Circular and elliptical CPW-fed slot and microstrip-fed antennas for ultrawideband applications. *IEEE Antennas Wireless Propag. Lett.*, **5** (2006), 294–297.
- [12] Ebrahimi, E.; Litschke, O.; Baggen, R.; Hall, P.S.: Isolation enhancement of planar disc antenna and ground plane in UWB applications. *Electron. Lett.*, **46** (23) (2010), 1539–1541.
- [13] Jung, J.; Choi, W.; Choi, J.: A small wideband microstrip-fed monopole antenna. *IEEE Microw. Lett.*, **15** (10) (2005), 703–705.
- [14] Jung, J.; Choi, W.; Choi, J.: A compact broadband antenna with an L-shaped notch. *IEICE Trans. Commun.*, **E89-B** (6) (2006), 1968–1971.
- [15] Ojaroudi, M.; Kohneshahri, G.; Noory, J.: Small modified monopole antenna for UWB application. *Microw. Antennas Propag.*, **3** (5) (2009), 863–869.

- [16] Kerkhoff, A.J.; Rogers, R.L.; Ling, H.: Design and analysis of planar monopole antennas using a genetic algorithm approach. *IEEE Trans. Antennas Propag.*, **52** (10) (2004), 2709–2718.
- [17] Ojaroudi, M.; Ghanbari, Gh.; Ojaroudi, N.; Ghobadi, Ch.: Small square monopole antenna for UWB applications with variable frequency band-notch function. *IEEE Antennas Wireless Propag. Lett.*, **8** (2009), 1061–1064.
- [18] Ray, K.P.: Design aspects of printed monopole antennas for ultra-wide band applications. *Int. J. Antennas Propag.*, **1** (2008), 1–8.
- [19] Agrawall, N.P.; Kumar, G.; Ray, K.P.: Wide-band planar monopole antennas. *IEEE Trans. Antennas Propagation*, **46** (2) (1998), 294–295.
- [20] Gautam, A.K.; Yadav, S.; Kanaujia, B.K.: A CPW-fed compact UWB microstrip antenna. *IEEE Antennas Wireless Propag. Lett.*, **12** (2013), 151–154.
- [21] Xu, K.; Zhu, Z.; Li, H.; Huangfu, J.; Li, C.; Ran, L.: A printed single-layer UWB monopole antenna with extended ground plane stubs. *IEEE Antennas Wireless Propag. Lett.*, **12** (2013), 237–240.
- [22] Sung, Y.: UWB monopole antenna with two notched bands based on the folded stepped impedance resonator. *IEEE Antennas Wireless Propag. Lett.*, **11** (2012), 500–502.
- [23] Venkata, S.K.; Rana, M.; Bakariya, P.S.; Dwari, S.; Sarkar, M.: Planar ultrawideband monopole antenna with tri-notch band characteristics. *Progr. Electromagn. Res. C*, **46** (2014), 163–170.
- [24] Rani, S.; Singh, Er., D.; Sherdia, K.: UWB Circular Microstrip Patch Antenna design simulation & its analysis. *Int. J. Adv. Res. Comput. Commun. Eng.*, **3** (7) (2014), 7519–7521.
- [25] Chen, Z.N.; See, T.S.P.; Qing, X.: Small printed ultrawideband antenna with reduced ground plane effect. *IEEE Trans. Antennas Propag.*, **55** (2) (2007), 383–388.
- [26] Chaturvedi, S.; Sharma, S.; Chaturvedi, S.; Sangal, S.; Sharma, S.: Ultra-wide bandwidth circular monopole antenna. *Int. J. Sci. Res. Eng. Technol.*, **1** (5) (2012), 279–282.
- [27] Ershadh, M.; Krishna, P.; Bhagyaveni; Subramanian, S.: Design of a novel antenna and its characterization in frequency and time domains for ultra wide band applications. *Progr. Electromagn. Res. C*, **48** (2014), 69–76.
- [28] Gao, G.-P.; Hu, B.; Zhang, J.-S.: Design of a miniaturization printed circular-slot UWB antenna by the half-cutting method. *IEEE Antennas Wireless Propag. Lett.*, **12** (2013), 567–570.
- [29] Quintero, G.; Zurcher, J.-F.; Skrivervik, A.K.: System fidelity factor: a new method for comparing UWB antennas. *IEEE Trans. Antennas Propag.*, **59** (7) (2011), 2502–2512.
- [30] Thwin, S.S.: Compact asymmetric inverted cone ring monopole antenna for UWB applications. *Progr. Electromagn. Res. Lett.*, **36** (2013), 57–65.



Sandeep Kumar Palaniswamy is currently working towards the Ph.D. degree at Anna University, Chennai, India. His research interests include wideband antennas and UWB antennas.



Malathi Kanagasabai was born in India. She completed her Ph.D. degree in microwave engineering from the Department of Electronics and Communication Engineering, College of Engineering Guindy, Anna University, Chennai. She is currently associate professor in the Department of Electronics and Communication Engineering, Anna University, Chennai. Her research interests include microwaves, transmission lines, antenna structures, and high speed systems.



Arun Kumar Shrivastav was born in India. He completed his Ph.D. degree from Department of Electronics and Communication Engineering, Anna University, Chennai. He is currently working as scientist F at Center for Electro Magnetics, Society for Applied Microwave Electronics Engineering and Research (SAMEER), Chennai, India. His research interests include microwaves, transmission lines, antenna structures, and high speed systems.